Geophys. J. R. astr. Soc. (1977) **51**, 431–452

Isostatic compensation on a continental scale: local versus regional mechanisms

R. J. Banks,* R. L. Parker and S. P. Huestis
Institute of Geophysics and Planetary Physics, University of California, San Diego, USA

Received 1977 March 17; in original form 1977 January 14

Summary. Using the techniques of linear and quadratic programming, it can be shown that the isostatic response function for the continental United States, computed by Lewis & Dorman (1970), is incompatible with any local compensation model that involves only negative density contrasts beneath topographic loads. We interpret the need for positive densities as indicating that compensation is regional rather than local. The regional compensation model that we investigate treats the outer shell of the Earth as a thin elastic plate, floating on the surface of a liquid. The response of such a model can be inverted to yield the absolute density gradient in the plate, provided the flexural rigidity of the plate and the density contrast between mantle and topography are specified.

If only positive density gradients are allowed, such a regional model fits the United States response data provided the flexural rigidity of the plate lies between 10^{21} and 10^{22} N m. The fit of the model is insensitive to the mantle/load density contrast, but certain bounds on the density structure can be established if the model is assumed correct. In particular, the maximum density increase within the plate at depths greater than 34 km must not exceed 470 kg m^{-3}; this can be regarded as an upper bound on the density contrast at the Mohorovicic discontinuity.

The permitted values of the flexural rigidity correspond to plate thicknesses in the range 5–10 km, yet deformations at depths greater than 20 km are indicated by other geophysical data. We conclude that the plate cannot be perfectly elastic; its effective elastic moduli must be much smaller than the seismically determined values. Estimates of the stress-differences produced in the earth by topographic loads, that use the elastic plate model, together with seismically determined elastic parameters, will be too large by a factor of four or more.

1 Introduction

Measurements of gravity over large-scale topographic features such as mountain ranges typically show negative Bouguer anomalies that have an inverse correlation with the

* Present address: Department of Environmental Sciences, University of Lancaster, Lancaster, England.

elevation. The recognition of this relationship led to the development of the concept of isostasy; that the excess mass above sea level represented by topographic features is compensated by a deficiency of mass below sea level. The hypothesis can be given a more specific formulation in one of two ways: either in terms of the equality of mass of material in equal prisms above the 'level of compensation', or in terms of the equality of hydrostatic pressure over a 'level' surface within the earth. The second is a more flexible condition, in that it can be applied to both local and regional compensation models, and only requires that stresses within the earth are hydrostatic below some depth.

The Bouguer gravity anomalies associated with topographic features contain information about the distribution of compensating mass, even though they do not determine it uniquely. If plausible limits can be placed on the maximum density differences involved, for instance, bounds can be established on the depth of the compensating mass (Parker 1975). More powerful constraints on the distribution of compensation are possible if a mechanical model of the compensation process can be specified.

The earliest, and still the most commonly used, isostatic models are those of Pratt and Airy. They have tended to dominate geophysical thinking about the processes by which isostasy is achieved, and about the definition and computation of isostatic gravity anomalies. Both are local compensation models: a topographic load is assumed to be supported only by the hydrostatic pressure at a point on the surface of compensation directly beneath it, or conversely, the compensating density at any point within the earth is determined only by the topographic elevation directly above it. The classic picture of local compensation is of a set of rigid blocks floating in a denser liquid, entirely independent of one another, and free to move vertically so as to achieve individual hydrostatic equilibrium. In the Pratt model, the blocks have different densities, the value of the density determining the elevation; in the Airy model, the blocks are of equal density, but different length. Consequently, the distributions of compensating density are different. In the Pratt model, it is distributed uniformly with depth down to the level of compensation, which is typically found to be 60–110 km. In the Airy model, the compensating density contrast occurs at the base of the block (at depths of 30–60 km), where the low-density material displaces the high-density fluid. A more general Airy model can be envisaged in which the density of the blocks changes continuously with depth, rather than there being a single jump at the base. In that case, the compensation will be distributed vertically beneath the topography, and for certain density distributions, will look like the Pratt model (Jeffreys 1970).

The difficulty with such local compensation models is that they involve unreasonable assumptions about the mechanical behaviour of the crust and upper mantle in response to surface loads. In the Airy model, for instance, any topographic load, however localized and however small its spatial scale, must give rise to vertical movements of the crust in order that local compensation be reachieved. Such a response implies that the crust has no strength at all for vertical loads. Movements along vertical fractures or some form of creep must take place in response to extremely small stress differences. Yet isostatic gravity anomalies with magnitudes of several hundred $\mu m\ s^{-2}$ and spatial scales of up to 100 km or more are common features of the continental crust. Such anomalies are often produced by igneous intrusions with well-determined ages that may exceed 100 Myr. Despite the length of time that has elapsed since their emplacement, they are still not locally compensated. The continued existence of the gravity anomalies implies that the crust is able to sustain stress differences of up to 100 kbar or more for a significant fraction of geological time.

Considerations of this kind have led geophysicists to investigate various forms of regional compensation. The mechanical model that has been most often used is one in which the outer shell of the earth is treated as a thin elastic plate, floating on the surface of a liquid.

Vening Meinesz (see Heiskanen & Vening Meinesz 1958) has used such a model as the basis for the computation of isostatic gravity anomalies. His approach was to calculate the distribution of compensation in a crustal column according to the Airy–Heiskanen scheme, then to redistribute the compensation laterally in accordance with the deformation that would be expected for an elastic plate subjected to the known topographic load. It does not seem to have been satisfactorily established that the fit of such a model to the data (as measured by the size of the residual isostatic anomalies) is any better than that of the local compensation models.

In this paper, we attempt to establish by formal statistical tests whether a local or regional compensation model is more satisfactory in accounting for the relationship between Bouguer gravity and topography determined over a region of continental scale. We agree with Jeffreys (1970) that 'the proper line of progress now is to start from what we know, namely, the heights and the values of gravity and try to find out what distributions of density underground are needed to explain them.' We do not share the pessimism of Hayford & Bowie (1912), when they say 'there is little hope of determining by the use of gravity observations the manner of the distribution of the isostatic compensation with respect to depth.'

The first steps along the lines proposed by Jeffreys were taken by Dorman & Lewis (1970, 1972) and Lewis & Dorman (1970), when they showed how to summarize in the most effective way the relationship between gravity and topography, by calculating an isostatic response function relating the gravity anomaly of the compensation to the elevation of topographic features of a given wavenumber. The isostatic response they computed was derived from data covering the whole of the continental United States. By averaging over an area of continental scale, they eliminated relationships between gravity and topography that are only applicable to specific geographical regions. We should not, therefore, expect to derive information from their response data about compensation processes that involve complex lateral variations in the structure of crust and upper mantle. Such processes may be important in a local context, but what we are concerned to discover is just how much of the compensation process is explicable in terms of a single model that is valid for an entire continent. From that point of view, the elimination of locally specific relationships between gravity and topography is a considerable advantage.

Dorman & Lewis (1970, 1972) show that their isostatic response estimates can be inverted to yield the compensating density distribution, provided local compensation is assumed. When they inverted the United States response, they found that the data required negative densities down to 150 km or so, and positive densities at greater depths. They accepted the positive densities as a genuine feature of the local compensation process; we prefer to interpret them as an indication that compensation is regionally rather than locally distributed. If this assumption is correct, tests of the statistical significance of the positive densities are equivalent to tests of the validity of the local compensation model. Using linear and quadratic programming techniques, we are able to show that the hypothesis that everywhere negative local compensation density models fit the data can be rejected at the 90 per cent level.

The regional compensation model that we then adopt in our attempts to satisfy the data is the thin elastic plate over a liquid. Its response can be inverted to yield the absolute density in the plate, provided the flexural rigidity of the plate and the density contrast between topography and mantle are specified. The model gives acceptable fits to the data provided the flexural rigidity and density structure of the plate lie within certain bounds. If the model is accepted as a realistic representation of the Earth, the bounds enable conclusions to be drawn about the rheology and density structure of the crust and upper mantle.

2 The isostatic response data

The isostatic model to which Lewis & Dorman fit their topographic and gravity data is

$$G(\mathbf{k}) = Q(k)H(\mathbf{k}) + N_G(\mathbf{k}) \tag{1}$$

$G(\mathbf{k})$, $H(\mathbf{k})$ are the two-dimensional Fourier Transforms of the Bouguer gravity and topographic maps respectively. The isostatic response function, Q, depends on the modulus k of the horizontal wavenumber $\mathbf{k}$. $Q(k)H(\mathbf{k})$ is the part of the Bouguer anomaly map at wavenumber $\mathbf{k}$ that can be attributed to the compensating density distribution. $N_G(\mathbf{k})$, the residual Bouguer anomaly, or 'isostatic anomaly', does not correlate on the average with $H(\mathbf{k})$, and is due to lateral density variations, mainly of relatively small scale, in the crust and possibly in the upper mantle.

The best estimate of $Q(k)$ is given by

$$Q(k) = \frac{\langle G(\mathbf{k})H^*(\mathbf{k})\rangle}{\langle H(\mathbf{k})H^*(\mathbf{k})\rangle} \tag{2}$$

where the brackets denote averaging of the cross spectrum and power spectrum around annuli in the wavenumber domain.

The assumptions that are inherent in this model are discussed by Dorman & Lewis (1970), Lewis & Dorman (1970) and Banks & Swain (1977). The relationship between gravity and topography is assumed to be linear. Dorman & Lewis point out that this is not exactly true for some isostatic models. In particular, the variation of the depth of the compensating density in the Airy model makes it non-linear, though only slightly so. The method used to stabilize the spectral estimates, forcing Q to be a function of $|\mathbf{k}|$, allows only isostatic models in which the compensation of a point topographic load is distributed with cylindrical symmetry beneath it. Neither of these assumptions is unduly restrictive.

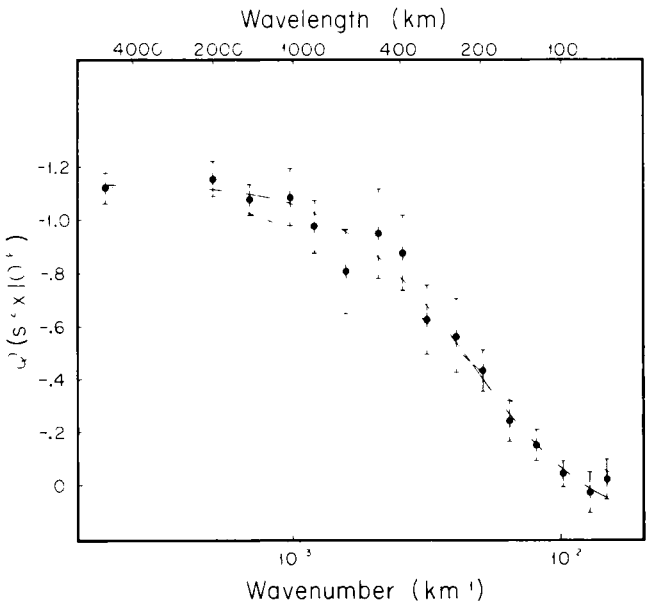

Figure 1. Isostatic response estimates for the United States. Bars represent ± 1 standard error in the data. Continuous curve is the response of the local compensation model with both negative and positive densities; dashed curve is the response of the local compensation model with only negative densities and smallest one-norm misfit to the data.

Fig. 1 shows the isostatic response estimates for the continental United States, as plotted by Dorman & Lewis (1972), together with their associated standard errors, which play an important role in the assessment of the goodness of fit of isostatic models. It should be noted that the size of the errors is, except at the shortest wavelengths, a measure of N_G, the component of the gravity spectrum not fitted by the linear model.

3 Local compensation

In the analysis of both local and regional compensation, we shall use a plane rather than spherical geometry. In the case of local compensation, it is just as easy to write down the isostatic response of the spherical earth model as that of the plane earth model (see Dorman & Lewis (1970, 1972) for details). However, the problem of the elastic deformation of the plate that must be solved in the analysis of regional compensation can be handled more easily using plane geometry, so we have chosen to work with a plane earth model throughout. This simplification leads to inaccuracies in the computation of the gravity anomalies associated with the compensation. However, it turns out that the maximum depth of the compensating density is small compared to the radius of the Earth. In consequence, the effect of the incorrect geometry on the response is generally smaller than the estimated errors in the data, except at the very longest wavelength (4096 km) where it is of comparable size.

3.1 RESPONSE OF THE LOCAL COMPENSATION MODEL

There is no necessity for a precise specification of the mechanical characteristics of the local compensation model – whether blocks of rigid lithosphere move along vertical faults, or deformation takes place by some form of creep, etc. All that we need require is that the compensating density contrast (relative to the normal earth) at any point within the earth is determined only by the elevation of the topography directly above it. In addition, the compensating density, ρ_c, must be a linear function of the topography $h(\mathbf{r})$ to produce a linear response; a density model that satisfies these criteria is

$$\rho_c(\mathbf{r}, z) = \rho(z) h(\mathbf{r}) \tag{3}$$

where $\mathbf{r}$ is the projection of the position vector on to the x, y plane, and $\rho(z)$ is the compensating density associated with unit topographic load.

Such a definition of the local compensation model is compatible with both the Pratt and Airy mechanisms. For the Pratt model, $\rho(z) = \rho_0/H_c$, where ρ_0 is the density of the topography, and H_c is the depth of the level of compensation. The compensation is uniformly distributed in the depth range $(0, H_c)$. In a simple Airy model, with compensation by variations in the thickness of the crust, the corresponding density anomalies can be replaced (in a linear approximation) by a distribution with the form of equation (3), in which $\rho(z)$ is a spike of magnitude ρ_0 in a layer of unit thickness, located approximately at the mean depth of the Mohorovicic discontinuity. More sophisticated forms of Airy compensation, involving the displacement of boundaries within the crust, or of regions with more gradual vertical density gradients, will give rise to corresponding structure in $\rho(z)$.

For complete local compensation, we must have

$$\int_0^\infty \rho_c(\mathbf{r}, z)\, dz = -\rho_0 h(\mathbf{r})$$

(the minus sign arises because $h(\mathbf{r})$ is measured positive upwards, z is positive downwards). The model defined by equation (3) satisfies this requirement provided

$$\rho_0 = -\int_0^\infty \rho(z)dz.$$

Dorman & Lewis (1970) show that the response of the local compensation model is

$$Q(k) = 2\pi\mathscr{G}\int_0^\infty \rho(z)\,\exp(-2\pi kz)\,dz \tag{4}$$

Hence

$$Q(0) = 2\pi\mathscr{G}\int_0^\infty \rho(z)\,dz$$

$$= -2\pi\mathscr{G}\rho_0$$

if the compensation is perfect. It follows that if we make use of an estimate of $Q(0)$ in inverting the data, we are in fact specifying the completeness of the compensation. Making a reliable estimate of $Q(0)$ may not be a straightforward matter (Banks & Swain 1977). The mean free air anomaly over the area analysed by Lewis & Dorman is 0.4 μm s^{-2}; the mean elevation is 684 m. These figures suggest that compensation is almost perfect, and that we ought to be able to set $Q(0) = -2\pi\mathscr{G}\rho_0 = -1.1190 \times 10^{-6}$ s^{-2} with very high accuracy. However, the mean Bouguer anomaly is -816.6 μm s^{-2}, corresponding to $Q(0) = -1.1934 \times 10^{-6}$ s^{-2}. The discrepancy might be caused by the spherical rather than the plane geometry of the compensation. We have attempted to allow for it by making a more liberal estimate of the uncertainty, setting $Q(0) = -(1.1190 \pm 0.04) \times 10^{-6}$ s^{-2}.

The integral in equation (4) is evaluated over a finite range of depth. The maximum depth, z_m, was chosen to be 400 km, and k and z were normalized in terms of z_m. Substituting $\kappa_j = k_j z_m$ (k_j is the wavenumber of the jth response estimate Q_j) and $\zeta = z/z_m$, we find

$$Q_j = 2\pi\mathscr{G}z_m\int_0^1 \rho(\zeta)\,\exp(-2\pi\kappa_j\zeta)\,d\zeta \qquad j = 1, M. \tag{5}$$

3.2 INVERSION OF THE RESPONSE ASSUMING LOCAL COMPENSATION

Equation (5) can be inverted for the density distribution $\rho(\zeta)$ using the spectral expansion method described by Parker (1977). The details of its application to the isostatic response problem are given by Banks & Swain (1977). The misfit of the theoretical response of a model to the observations is traded-off against the errors in the inverted density distribution. If too good a fit is required, these errors become unacceptably large and the model is meaningless. The model that we selected by this procedure has a squared two-norm misfit to the data of $\chi^2 = 3.92$. It is shown in Fig. 2, together with the associated standard errors. The effective number of degrees of freedom is 13, so that the model is acceptable at better than the 99 per cent level.

Two points should be borne in mind in assessing the model plotted in Fig. 2. First, that it is a highly smoothed version of the actual density distribution. Second, that $\rho(z)$ is the compensating density for 1 m of topography. To obtain the actual density changes, $\rho(z)$ must be multiplied by the elevation. Thus topography 1000 m high would require density reductions of as much as 100 kg m^{-3} for its compensation.

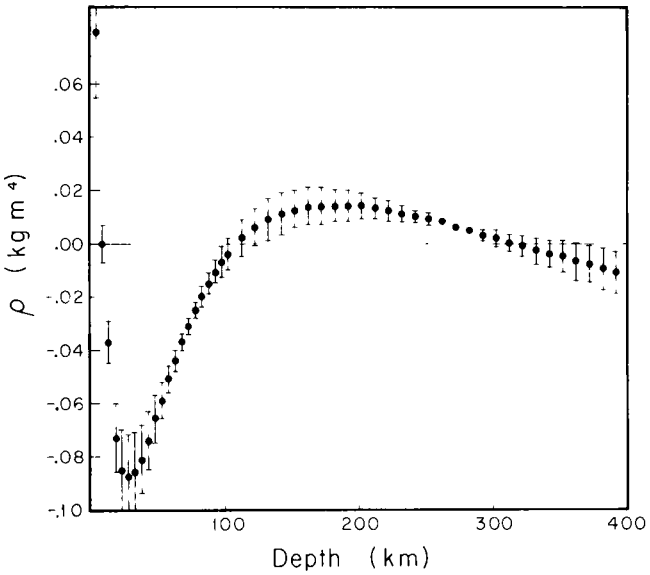

Figure 2. Isostatic density model for the USA, obtained by inverting the response data in Fig. 1, assuming local compensation. Ordinate is density contrast per unit topographic elevation.

The essential features of the density model are a negative density lobe at depths of 10–100 km, and a positive lobe at depths of 100–300 km. Mass deficiencies to compensate the excess mass above sea level are a necessary feature of all isostatic models. However, it is usually assumed that only density reductions are involved, not positive densities as well. Dorman & Lewis (1972) also found that they needed positive densities to fit their response data. They accepted them as an integral part of the compensation mechanism, and attempted to substantiate them by comparing their density model with differences between seismic velocity structures beneath regions of the United States with high and low mean elevations. However, a second interpretation of the positive densities is possible: that the local compensation model is not valid. As Jeffreys (1970) has pointed out, any density distribution derived under the assumption of local compensation can be replaced by a lateral distribution at shallower depths that produces exactly the same gravity anomaly. Such a lateral distribution in response to a localized load constitutes regional compensation. Thus, it is certainly possible to replace a local compensation model that involves positive densities by a regional compensation model that only involves negative densities. Such a model must fit the response data equally well, though the problem remains whether any reasonable mechanical model of the Earth's response to surface loads can give rise to the required lateral density changes.

Hence, if we can demonstrate that the positive density lobe is an essential feature of the local compensation model, it must follow that either (a) positive density changes really exist or (b) compensation is regional rather than local.

3.3 TESTING THE SIGNIFICANCE OF THE POSITIVE DENSITIES

The errors shown in Fig. 2 do not completely specify the uncertainty in the density distribution. The inverted model is a highly smoothed version of the true density structure, obtained by convolving it with certain kernels. The shape of the kernels determines how well structure at a given depth is resolved, and whether the smoothed density estimates are appropriate

to the depth to which they are attributed. Dorman & Lewis (1972) have computed the resolving kernels associated with their United States response data. They are broad (50–100 km in width for structure in the depth range 0–100 km), so that the vertical resolution is poor, and they are asymmetric; the peaks are displaced from the depth at which the density contrasts actually occur. These features indicate that it is unlikely to be profitable to approach the problem of the significance of the positive densities by way of the resolving kernels.

The resolving kernels attempt to give answers to very specific questions about the density structure. The information content of the data is quite inadequate to supply these answers. However, for our purposes, all that is required is the answer to a much more general question: is a model that involves only negative densities compatible with the data? More specifically, what we wish to know is the confidence level at which we can reject the hypothesis that the data were generated by a structure involving only negative densities.

To do this we first construct the entirely negative model fitting the data best; for the moment we shall suppose that χ^2, the standard statistic, measures the mismatch between model and observation. We then hypothesize that the best-fitting model is indeed the true structure, and now we calculate the probability that the misfit would be as big or bigger than the one observed, given the standard errors in the data. If this probability is very small, we may reject the hypothesis and, more important, we can reject a similar hypothesis concerning any other everywhere-negative model, because this was the best-fitting model of its kind.

The computation of the probability is explained best by examination of a simple two-data problem (see Fig. 3), in which the two-dimensional data plane can be readily depicted. The set of data compatible with entirely negative models is the shaded wedge which is the mapping of the set of points $\rho(z) \leqslant 0$ on to Q_1, Q_2 via the functionals (4). Because no such model satisfies the data exactly, the actual observations lie outside the wedge at D; the hypothetical structure gives rise to data at B. Since we have normalized Q_1 and Q_2 by their standard errors, circles in this plane represent contours of equal χ^2; the probability that the observed misfit be as bad or worse than that observed is clearly the integral of the probability density function of the misfit measure over the whole plane outside the circle centre B radius BD. It can easily be confirmed that this is the standard χ^2_ν integral with $\nu = 2$. For N data, ν will be equal to N.

The discussion in this section has shown that two problems are involved in testing the hypothesis that positive densities are a necessary feature of local compensation models: finding the everywhere negative model with the smallest misfit to the data, and defining and evaluating the characteristics of the probability distribution of the chosen measure of misfit.

3.4 THE APPLICATION OF LINEAR AND QUADRATIC PROGRAMMING

If the chosen measure of misfit is a linear function of the observed and theoretical responses, the problem of finding the everywhere negative model with the smallest misfit to the data can be solved by linear programming. If a quadratic measure such as χ^2 is used, quadratic programming techniques are required.

The way in which the linear programming problem is set up is described by Banks & Swain (1977); see also Gass (1975). As in that paper, the measure of misfit we use is the one norm; the sum of the absolute values of the individual misfits:

$$\gamma = \sum_{j=1}^{M} |(Q_j - T_j)/\sigma_j|$$

Q_j is the observed value of the response, T_j the theoretical value for a particular model, and σ_j the standard error of the jth estimate. With this choice of misfit measure, the contours or surfaces of constant misfit in data space are diamonds or cross polytopes rather than circles or hyper-spheres, but otherwise the approach discussed in Section 3.3 remains the same.

The model is parameterized by dividing the slab $z = 0, z_m$ into layers of uniform density:

$$\rho(\zeta) = \rho_l \qquad \zeta_l < \zeta < \zeta_{l+1} \qquad l = 1, L$$

so that the theoretical response is given by

$$T_j = \sum_{l=1}^{L} V_{jl}\rho_l$$

where

$$V_{jl} = \frac{\mathcal{G} z_m}{\kappa_j} \exp(-2\pi\kappa_j\zeta_l)\{1 - \exp[-2\pi\kappa_j(\zeta_{l+1} - \zeta_l)]\}.$$

The model is required to fit the data with misfit e_j, i.e.

$$(Q_j - T_j)/\sigma_j = e_j$$

and the model that we seek is that with the minimum value of

$$\sum_{j=1}^{M} |e_j|.$$

The densities ρ_l are all constrained to be negative, and, in addition, bounds are placed on the depth-integrated density

$$\sum_{l=1}^{L} \rho_l(\zeta_{l+1} - \zeta_l) z_m.$$

For perfect local compensation, this sum should be equal (and opposite in sign) to the topographic density ρ_0. Exact equality is not desired; ρ_0 is not known exactly, and some measure of under or over-compensation may be allowable. The constraint was relaxed by requiring that the sum, or ρ_0, lie in the range 2500–2700 kg m^{-3}.

z_m was chosen to be 100 km, and the slab divided into 20 equal layers (initial tests showed that non-zero densities below 100 km were not required). The solution with the minimum one-norm misfit to the data, and which satisfies the above constraints, turned out to have only one non-zero component: the compensating density in the layer between 30 and 35 km depth was -0.540 kg m^{-4}. Note that this solution corresponds to the upper bound on the crustal density; the lower bound is redundant. Reducing the upper bound must make the misfit worse. The misfit of this model is $\gamma_m = 15.766$.

The second part of the problem is to evaluate the probability P that the one-norm exceeds this value. Tables of the probability density function for the one-norm have been computed for values of M up to 10, using the method described by Hartley (1945) and Hartley & Godwin (1945). We find that, with 10 or more data, γ can be treated as a normally distributed variable with mean $\bar{\gamma} = M(2/\pi)^{1/2}$ and standard deviation $s = [M(1 - 2/\pi)]^{1/2}$. Then the probability that the one-norm of M data exceeds γ_m is

$$P\{\gamma > \gamma_m; M\} = 1 - \frac{1}{\sqrt{2\pi}} \int_{-\infty}^{X} \exp(-X^2/2)dX$$

where

$$X = (\gamma_m - \bar{\gamma})/s.$$

In this case, $P\{\gamma > 15.77; 16\} = 0.11$. It follows from the discussion in Section 3.3 that the hypothesis that the data are compatible with an everywhere negative model can be rejected at the 89 per cent level.

The level of confidence is quite sensitive to the choice of upper bound on the topographic density; for example, if ρ_0 is allowed to be as large as 2800 kg m^{-3}, the confidence level is reduced to 59 per cent.

The responses of the model obtained by inversion, and of the all-negative model with minimum misfit, are plotted in Fig. 1 for comparison with the observations. The fit of the two-sign model is obviously very good; that of the all-negative model is poor. Although the misfits of individual points are never very large, they show a consistent behaviour with wavenumber that would not be judged acceptable on the basis of a visual appraisal. At wavelengths greater than 200 km the misfits are consistently negative, while below 200 km they are consistently positive. The overall shape of the response curve is clearly incorrect. The difficulty in achieving a satisfactory fit arises because d^2Q/dk^2 never changes sign for all-negative local compensation models, although the data obviously require such a change (this is not obvious in Fig. 1 because of the logarithmic wavenumber scale).

Quadratic programming was used to find the model with the smallest χ^2 misfit, subject to the same constraints imposed in the linear case. The minimum misfit models were identical; χ^2_m was 20.86. It turned out, in this case, that the squared two-norm misfit did not discriminate more strongly than the one norm against the hypothesis of negativity.

3.5 GEOPHYSICAL SIGNIFICANCE OF THE EVERYWHERE NEGATIVE MODEL

We have shown that no local compensation model that involves only negative densities fits the observations adequately. However, the best-fitting negative model is of considerable interest. If the layer thickness is 5 km, non-zero densities are only required in the layer at 30–35 km depth. The model may be refined by introducing thinner layers in this depth range. However, when this is done, the minimum misfit model is still found to have finite densities only in one layer (or sometimes in two adjacent layers). It is clear that the optimum negative model is a delta function, at a depth of 32 km.

Such a distribution of density is obviously incompatible with the Pratt mechanism of compensation. Forcing the compensation to be uniformly distributed with depth would lead to a worse misfit to the data. The form of $\rho(z)$ for the optimum local compensation model clearly corresponds to that we would expect from the linear approximation to the Airy mechanism. The depth of the density spike corresponds very well to usually accepted estimates of the mean thickness of the continental crust, as determined by seismic refraction measurements. The implication, if we chose to ignore the misfit to the data, would be that local compensation was achieved by lateral variations in the thickness of the crust.

The approach we took in Section 3.3 in setting up the statistical tests can be used to throw an interesting light on the question of why Airy compensation at a single depth emerges as the best-fitting local compensation model. In the previous discussion of Fig. 3, we ignored the structure of the density model. Let us suppose that the density distribution is parameterized by dividing the slab $(0, z_m)$ into L layers. The L constraints generated by requiring the density of each of these layers to be negative, define L hyperplanes in data space; projected on to a two-dimensional data space, they appear as L lines through 0, such as $0C_1$, $0C_2$, etc. However, for the purpose of measuring the minimum distance of a

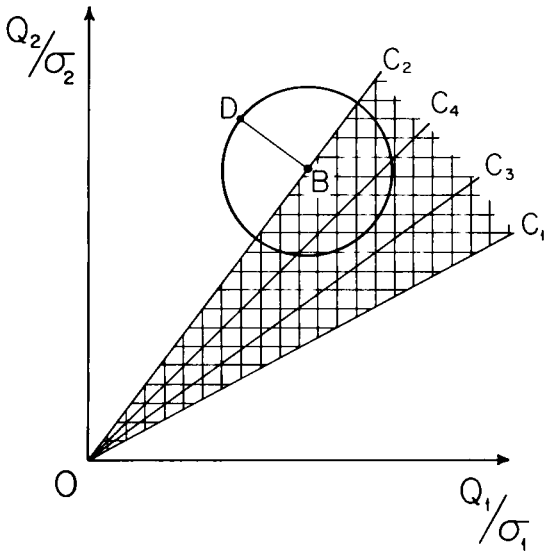

Figure 3. Schematic diagram to illustrate misfit of negative density local compensation models (shaded region) to response data. For explanation, see Section 3.3 of the text.

point such as D from the region of negative models (i.e. the misfit of the data to the best-fitting negative model), we are only interested in the lines $0C_1$ and $0C_2$ that bound the area containing all the others such as $0C_3$ and $0C_4$.

As the two-data example shows, if the everywhere negative model does not fit the data, i.e. if D lies outside the shaded region, the best fitting model B must lie on one of the lines $0C$. But these lines are the projections of the axes in model space defined by $\rho_l = \rho' \ (l = l')$, $\rho_l = 0 \ (l \neq l')$. B has only one non-zero component. In the limit as the number of layers becomes large, the minimum misfit model will be a delta function. It follows that, simply because the negative local compensation model is inadequate, any attempt to interpret gravity and topographic data using such a model will yield, as the best-fitting model, Airy compensation at a single depth.

A complication arises when the isostatic constraint is also imposed. An upper and a lower bound is placed on a linear combination of the densities ρ_l. These bounds define two extra hyperplanes that further limit the convex set of allowable models. If the isostatic constraint is applied, the minimum misfit model could lie on one of these planes. In that case the best-fitting model would have a number of non-zero components. This is not observed in the local compensation problem, but does appear to arise in the case of regional compensation.

Since all forms of local compensation involving only negative densities are rejected by the statistical tests, we are forced to turn to other compensation mechanisms. We could accept the reality of the positive densities, but we prefer first to investigate the possibility of explaining the response in terms of a regional compensation model.

4 Regional compensation

4.1 A SIMPLE REGIONAL COMPENSATION MODEL

Vening Meinesz (see Heiskanen & Vening Meinesz 1958), Walcott (1970, 1976), and McKenzie & Bowin (1976), among others, have interpreted the gravity anomalies associated

with topographic loads in terms of regional compensation. The rheological models which they assume in order to compute the deformation produced by topographic loading are essentially identical. The outer shell of the Earth is treated as an elastic plate floating on the surface of a liquid. In the context of this discussion of regional compensation, the plate will be referred to as the lithosphere, and the liquid as the asthenosphere. The details of the model are shown in Fig. 4. To illustrate how regional compensation is effected, the response of the lithosphere to a spatially localized topographic load is shown. Although short wavelengths dominate the spectrum of the load topography, they are suppressed in the spectrum of plate deformation, and long wavelengths dominate there. In spatial terms, the concentrated load is supported over an area considerably greater than its own extent by the buoyancy forces set up on the base of the plate.

A reasonable case can be made for such a rheological model of the Earth's response to stresses acting over periods of 10^4–10^8 yr. The outermost shell deforms by brittle fracture and possibly transient creep, but otherwise behaves elastically. At depths greater than 20 km or so, where the temperature exceeds half the melting temperature of the rocks, steady state (viscous) creep becomes the dominant process of deformation, and the Earth can be treated as a very viscous liquid. It should be emphasized that the use of the terms lithosphere and

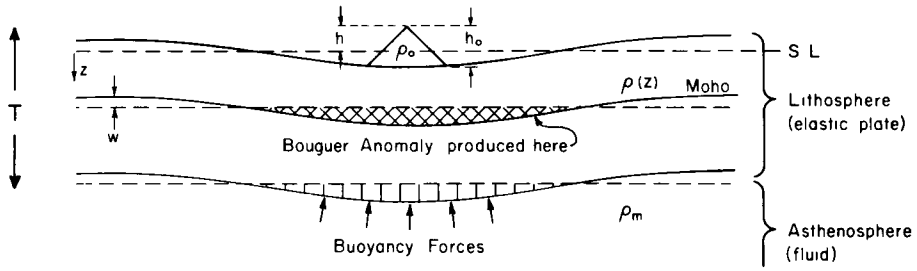

Figure 4. The regional compensation model.

asthenosphere for the elastic plate and fluid does not imply a correspondence to the 'lithosphere' and 'asthenosphere' of plate tectonic terminology. In the context of plate tectonics, the properties of the plates are usually assumed to be those determined from seismic measurements, i.e. from the elastic response of the Earth to stresses lasting at most a day or so. The response to the long term stresses involved in topographic loading may be completely different. We should not assume any *a priori* knowledge from the seismic measurements about the thickness and 'elastic' properties of the plates involved in regional compensation.

The gravity anomalies that correlate with the topography are attributed to the bending of the lithosphere. It is obvious that density anomalies will be produced at horizontal boundaries where there is a discrete change in density (for example the Mohorovicic discontinuity). However, any region of the lithosphere in which the vertical density gradient is non-zero will, upon deformation, give rise to density anomalies and corresponding gravity anomalies. For simplicity, in Fig. 4 we only show the density anomaly created by the deformation of the Moho (assuming it to lie within the plate).

Walcott (1976) has compared the response of this regional compensation model to Dorman & Lewis' United States response data, but for some reason he assumes that all the gravity anomalies originate from sources at the surface of the plate. We shall not impose any constraint of this kind on our model, but allow sources at all depths within the plate.

4.2 THE RESPONSE OF THE PLATE-LOADING MODEL

The evaluation of the isostatic response of the plate loading model involves three steps:

(i) The determination of the plate deformation $w(\mathbf{r})$ in response to topographic load $\rho_0 g h_0(\mathbf{r})$.
(ii) The calculation of the density perturbation, $\Delta\rho(\mathbf{r}, z)$, produced by the deformation of the plate.
(iii) The calculation of the gravity anomaly caused by the density perturbation.

4.2.1 Calculation of the plate deformation

We shall treat the lithosphere as a thin elastic plate; that is, one whose thickness is small compared with the wavelength of the deformation. McKenzie & Bowin (1976) give a two-dimensional treatment of the thick plate problem, and point out the errors introduced by the thin plate assumption. However, in the isostatic response problem, the inaccuracies in the data at the short wavelengths are the limiting factor, rather than the errors arising from the thin plate approximation.

The equation for the equilibrium of the deformed plate is (see, e.g. Jeffreys 1970)

$$D \cdot \nabla^4 w(\mathbf{r}) = p(\mathbf{r}) \tag{6}$$

$w(\mathbf{r})$ is the upward deflection of the plate. Strictly speaking, it is the deformation of the median plane within the plate, but in the thin plate it will be assumed that all surfaces, including the top and bottom, deform similarly. $p(\mathbf{r})$ is the net upward force per unit area acting on the plate; it is generated by the topographic load $h_0(\mathbf{r})$ (density ρ_0) and the buoyancy force set up on the base of the plate by the displaced asthenosphere (density ρ_m), i.e.

$$p(\mathbf{r}) = -\rho_0 g h_0(\mathbf{r}) - \rho_m g w(\mathbf{r}). \tag{7}$$

The measured topography comprises two parts; the load topography and the plate deformation:

$$h(\mathbf{r}) = h_0(\mathbf{r}) + w(\mathbf{r}) \tag{8}$$

D is the so-called flexural rigidity of the plate. If the plate is continuous, homogeneous, and elastic, D can be expressed in terms of its thickness and of the elastic moduli of the material that constitutes it. The relationship is

$$D = \frac{ET^3}{12(1-\sigma^2)} \tag{9}$$

where T is the plate thickness, E is Young's Modulus, and σ is Poisson's Ratio. However, an alternative is to regard D as an experimentally determinable measure of the deformability or stiffness of the plate, irrespective of whether we choose to interpret it in terms of an elastic model, using equation (9). The ultimate interpretation of the measured value of D will depend on the rheological model of the lithosphere that is preferred.

The analysis is very much simplified by taking the two-dimensional Fourier Transforms of equations (6), (7) and (8). Then we find

$$(2\pi k)^4 D W(\mathbf{k}) = -\rho_0 g H_0(\mathbf{k}) - \rho_m g W(\mathbf{k}) \tag{10}$$

where

$$W(\mathbf{k}) = \int_S w(\mathbf{r}) \exp(i2\pi\mathbf{k}\cdot\mathbf{r})\, dS$$

etc. When $H_0(\mathbf{k})$ is eliminated by using equation (8), the relationship between the plate deformation $W(\mathbf{k})$ and the measured topography $H(\mathbf{k})$ that results is

$$W(\mathbf{k}) = -\left(\frac{\rho_0}{\rho_m - \rho_0}\right)\left(1 + \frac{16\pi^4 k^4 D}{(\rho_m - \rho_0)g}\right)^{-1} H(\mathbf{k}) \tag{11}$$

4.2.2 Calculation of the density perturbation

The density perturbation produced in a medium of density $\rho(\mathbf{r}, z)$ by a displacement field $\mathbf{u}(\mathbf{r}, z)$ is

$$\begin{aligned}\Delta\rho(\mathbf{r}, z) &= \operatorname{div}(\rho(\mathbf{r}, z)\mathbf{u}(\mathbf{r}, z)) \\ &= \rho(\mathbf{r}, z)\operatorname{div}\mathbf{u}(\mathbf{r}, z) + \mathbf{u}(\mathbf{r}, z)\cdot\nabla\rho(\mathbf{r}, z).\end{aligned}$$

We shall assume that the plate is effectively incompressible by putting $\operatorname{div}\mathbf{u}(\mathbf{r}, z) = 0$. Furthermore, the normal density distribution in the plate will be assumed to be a function only of depth. In that case

$$\Delta\rho(\mathbf{r}, z) = w(\mathbf{r})\frac{\partial\rho(z)}{\partial z} \tag{12}$$

where the vertical component of the displacement is assumed to be the same at all depths in the plate. We shall require the two-dimensional Fourier Transform of equation (12); it is

$$\Delta\rho(\mathbf{k}, z) = W(\mathbf{k})\frac{\partial\rho}{\partial z} \tag{13}$$

4.2.3 The gravity anomaly and the response

The approach taken by Parker (1973) can be used to write down the Fourier Transform of the gravity anomaly produced by the density perturbation $\Delta\rho(\mathbf{k}, z)$. It is

$$G(\mathbf{k}) = 2\pi\mathscr{G}\int_0^\infty \Delta\rho(\mathbf{k}, z)\exp(-2\pi kz)\,dz \tag{14}$$

and when the substitution is made from equation (13), we find

$$G(\mathbf{k}) = 2\pi\mathscr{G}W(\mathbf{k})\int_0^\infty \frac{\partial\rho}{\partial z}\exp(-2\pi kz)\,dz. \tag{15}$$

When the deformation $W(\mathbf{k})$ predicted in equation (11) by the thin plate theory is substituted into equation (15), the isostatic response function can be written down directly:

$$Q(k) = -2\pi\mathscr{G}\left(\frac{\rho_0}{\rho_m - \rho_0}\right)\left(1 + \frac{16\pi^4 k^4 D}{(\rho_m - \rho_0)g}\right)^{-1}\int_0^\infty \frac{\partial\rho}{\partial z}\exp(-2\pi kz)\,dz. \tag{16}$$

If a new response function is defined by

$$R(k) = -Q(k)\left(\frac{\rho_m - \rho_0}{\rho_0}\right)\left(1 + \frac{16\pi^4 k^4 D}{(\rho_m - \rho_0)g}\right) \tag{17}$$

it can be written as

$$R(k) = 2\pi\mathscr{G}\int_0^\infty \frac{\partial\rho}{\partial z}\exp(-2\pi kz)\,dz. \tag{18}$$

The form of equation (18) is identical to that of equation (4), the response of the local compensation model. However, the property of the Earth that determines the response is now the absolute vertical density gradient in the lithosphere, rather than a compensating density contrast relative to the normal structure. If $R(k)$ can be determined from the measured response $Q(k)$, it can be inverted for $\partial\rho/\partial z$ using exactly the same techniques as were employed in the analysis of the local compensation model.

4.3 ESTABLISHING BOUNDS ON D AND ρ_m

Direct inversion of the response $Q(k)$ assuming local compensation did not lead to very concrete conclusions about the density distribution, because of the poor resolution of the kernels, and it is unlikely that more satisfactory results would be achieved by inverting equation (18). The linear programming approach proved to be much more fruitful, and we turn to it immediately in attempting to establish whether a regional compensation model involving a plausible density distribution and plausible values of D, ρ_m etc. is compatible with the data.

As before, we parameterize the model, replacing the continuous density gradient $\partial\rho/\partial z$ by a series of discrete density jumps $\Delta\rho_l$ located at depths $z_l, l = 1, L$. The response of such a model is

$$R(k) = 2\pi\mathcal{G}\sum_{l=1}^{L}\Delta\rho_l \exp(-2\pi k z_l). \tag{19}$$

Non-zero density jumps are limited to the finite depth range $(0, z_m)$; and the wavenumbers and depths are normalized in terms of z_m. The theoretical response at the jth wavenumber can be written as

$$T_j = \sum_{l=1}^{L} V_{jl}\Delta\rho_l$$

where

$$V_{jl} = 2\pi\mathcal{G}\exp(-2\pi\kappa_j\zeta_l).$$

The linear programming problem is set up in much the same way as before. Constraints must be placed on the class of acceptable density models; otherwise the inverted structure, because it attempts to fit the inaccurate data exactly, will be geophysically meaningless. In the local compensation problem, we constrained the density contrast to be negative at all depths, and found the minimum misfit model. A comparable constraint on the regional compensation model is to require that the density gradient be positive at all depths, i.e. we seek the minimum misfit model (in the one-norm sense) subject to the set of constraints $\Delta\rho_l \geqslant 0, l = 1, L$. A reasonable case can be made for the imposition of this constraint on theoretical models. Density models derived from seismic velocities typically show positive density gradients in the crust and upper mantle down to 200 km depth. Density inversions may occur in the crust, but they are unlikely to be of very great vertical extent. Their effect on the response will consequently be small, since the contributions from the top and bottom of the layer will almost cancel. In any case, we can take positive density gradients as a working hypothesis, and use the response data and the regional compensation model as a means of testing its validity.

The principal difficulty in setting up the linear programming problem is that the data to be inverted are not the observed responses, Q_j, but the modified responses R_j. The derivation of R_j from Q_j requires knowledge of D, ρ_m, and ρ_0. For consistency, the topographic density

ρ_0 should be the standard density of 2670 kg m^{-3}, used in the reduction of the gravity data to Bouguer anomalies. We would prefer to derive the other two parameters, D and ρ_m, from the data, rather than assign to them some arbitrary values based on other geophysical arguments. The obvious way around the difficulty is to find the minimum misfit model for each pair of values, D and ρ_m. It may then be that the misfit is always unacceptable, for any plausible combination of D and ρ_m. In that case, we may conclude either that the regional compensation model is incorrect, or that density decreases are also required. If, on the other hand, the minimum misfits are acceptable for certain values of D, ρ_m, bounds on these quantities can be established, provided that we accept the correctness of the regional compensation model, and of the hypothesis that density always increases with depth.

With this approach, some care is necessary to ensure that the constraints are mutually consistent. Once ρ_m and ρ_0 have been fixed, the density distribution should be chosen to satisfy the constraint.

$$\rho_t = \sum_{l=1}^{L} \Delta\rho_l = \rho_m - \rho_0. \tag{20}$$

The imposition of such a constraint on ρ_t is equivalent to requiring perfect compensation at zero wavenumber. However, the two requirements, of isostasy and self-consistency, must be carefully distinguished. In order to separate them, it is preferable to introduce isostasy as a piece of observational data. The fact that the mean free air gravity anomaly is close to zero establishes the value of $Q(0)$, as explained earlier. To achieve self-consistency, once ρ_m and ρ_0 are chosen, the density models are also required to satisfy equation (20).

z_m was chosen to be 40 km after tests showed that non-zero densities at greater depths were not required by the data. The model consisted of the unknown density jumps $\Delta\rho_l$ at 2 km intervals from sea level to 40 km depth. Models with the minimum one-norm

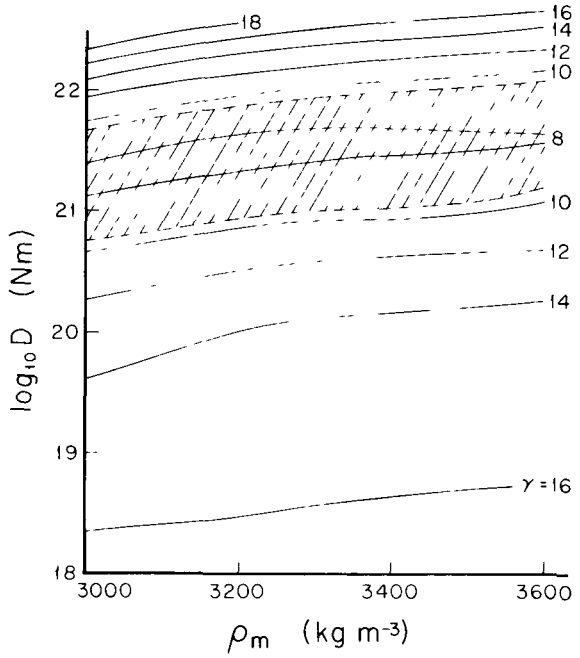

Figure 5. Contours of the minimum misfit of the regional compensation model, plotted as a function of the flexural rigidity of the plate (D), and the mantle density ρ_m.

misfit were found for pairs of values of D and ρ_m lying in the ranges $10^{16} \leqslant D \leqslant 4 \times 10^{22}$ N m and $3000 \leqslant \rho_m \leqslant 3600$ kg m^{-3}. In Fig. 5, contours of the minimum misfit are plotted as a function of $\log_{10} D$ and ρ_m. They are approximately parallel to the ρ_m axis, indicating that the misfit is effectively independent of the value of ρ_m over the range of values investigated. It is, however, sensitive to changes in D; the misfit surface is an asymmetric trough, asymptotically approaching a value of 16.6 as D tends to zero, and increasing very rapidly once D exceeds 10^{22} N m.

The hypothesis to be tested is that regional compensation models with everywhere positive density gradients can be rejected, provided D and ρ_m lie outside certain limits. With 17 data, in order that the probability P should be less than 0.1, the one-norm misfit must exceed 16.75. Thus, if the hypotheses of regional compensation and positive density gradients are accepted, values of D and ρ_m corresponding to models lying outside the 16.75 contour can be rejected at the 90 per cent level. Fig. 5 shows that values of D greater than 4×10^{22} N m can be rejected at this level. It is not possible to reject low values of D at the 90 per cent level. As D tends to zero, the regional compensation model becomes the original local compensation model that was rejected at just less than the 90 per cent level. If the confidence level is reduced to 80 per cent, the required misfit is 15.66. Values of D less than 4×10^{18} N m can be rejected at this level.

When we turn from judging our ability to reject a model, to judging its acceptability, an additional problem is created. The measure of the overall misfit between model and data that we use may not discriminate against certain forms of misfit. In particular, a measure like the one-norm does not discriminate strongly against models for which the individual misfits show consistent runs of a particular sign. This creates no difficulty when the hypothesis we are testing is that a model can be rejected; it merely means that the model can be rejected at a higher confidence level than we claim. However, when a model is being tested for its acceptability, the reverse is true. The result is that a model that is apparently acceptable at the 80 per cent level, say, on the basis of the probability estimate P, may look completely unacceptable when subjected to a visual comparison with the data. In Fig. 6, the responses of two models are compared with the data. They have misfits of 11.47 and 9.48, which would be judged acceptable at the 80 and 95 per cent levels respectively on the basis of P. Neither is completely satisfactory, in that the residuals tend to be consistently negative. What is needed for a visually satisfactory fit are randomly distributed residuals that do not correlate with their neighbours. Although the apparent difference between the two responses is slight, the 95 per cent acceptable model represents a significant improvement in this respect. On the basis of such arguments, we decided that, to be acceptable, a model should have a misfit of less than 9.48. The shaded area in Fig. 5 delineates the region of such models, and defines the range of acceptable values of D and ρ_m. ρ_m is unbounded, whereas D is quite tightly constrained to the range $10^{21} \leqslant D \leqslant 10^{22}$ N m.

The inability of the data to set tighter bounds on ρ_m can be explained by considering the following form of the response:

$$Q(k) = -2\pi\mathcal{G}\rho_0 \left\{1 + \frac{16\pi^4 D k^4}{(\rho_m - \rho_0)g}\right\}^{-1} \sum_{l=1}^{L} \left[\frac{\Delta\rho_l}{\rho_m - \rho_0}\right] \exp(-2\pi k z_l)$$

The value of ρ_m inside the square brackets does not affect the ability of $Q(k)$ to match the data. The misfit is determined by the ratio $\Delta\rho_l/(\rho_m - \rho_0)$, and $\Delta\rho_l$ can be adjusted to correspond to a chosen value of ρ_m. The other influence of ρ_m on the misfit is through the term in the curly brackets. D and $(\rho_m - \rho_0)^{-1}$ are equivalent in their influence on the response. D can vary over 20 orders of magnitude, and is only determined to one order of magnitude accuracy. $\rho_m - \rho_0$ must likewise change by an order of magnitude to affect the

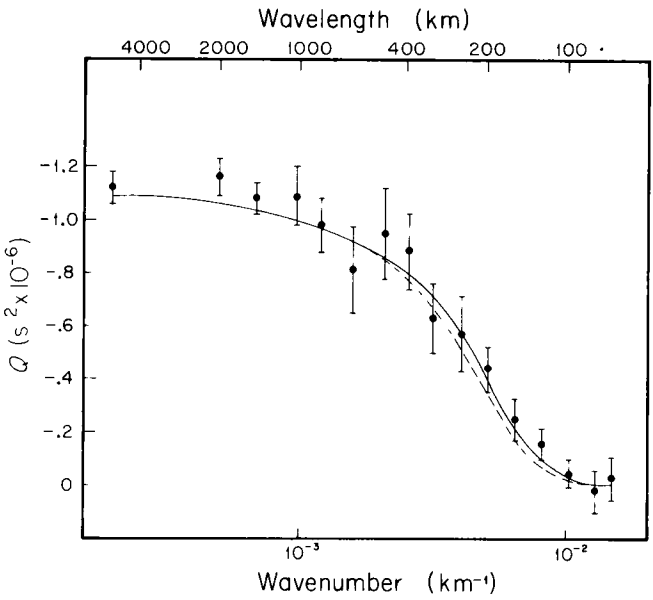

Figure 6. Fit of regional compensation models to the response data. Both models maximize the density below 26 km. Fits to the data are 80 per cent (dashed curve) and 95 per cent (continuous curve) acceptable.

response significantly. This means that ρ_m would have to drop below 2800 kg m^{-3} before the misfits became unacceptable.

4.4 BOUNDS ON DENSITY STRUCTURE

In Section 4.3 we were able to show that the class of regional compensation models that involved only positive density gradients contained a subset that satisfied the observational data at an acceptable confidence level. Allowed values of D are in the range 10^{21}–10^{22} N m; any reasonable value of ρ_m is possible, and we may certainly choose the generally accepted value of 3300 kg m^{-3}.

However, no other characteristic of the subset of acceptable models has as yet been specified. It may be that none of the models has a density structure that is compatible with other geophysical data, derived, for instance, from seismology. Alternatively, if seismic data can be used to constrain features of the model, it may be possible to draw stronger conclusions about acceptable values of D, or acceptable density structures. Our approach to this problem is to define features which all 'acceptable' models share in common. All 'acceptable' models are required to have a one-norm misfit that is less than a specified value. With this as one of the constraints, the linear programming problem is to find the model that has the smallest or greater total density in a given range of depths. In this way, bounds can be established on the density distributions of all 'acceptable' models. Of course, the procedure must be repeated for all values of D in the range 10^{21}–10^{22} N m.

An interesting problem is to try to determine the part played by the Mohorovicic discontinuity in isostatic compensation, and the magnitude of the density contrast between crust and mantle. Compilations of the depth of the Moho beneath continental crust that is at or near sea level show a wide scatter. Woollard (1970) gives 33 ± 7 km as the depth. It is certainly extremely rare for seismic refraction experiments on normal continental crust to yield Moho depths of less than 26 km. We can therefore begin our attempts to set bounds

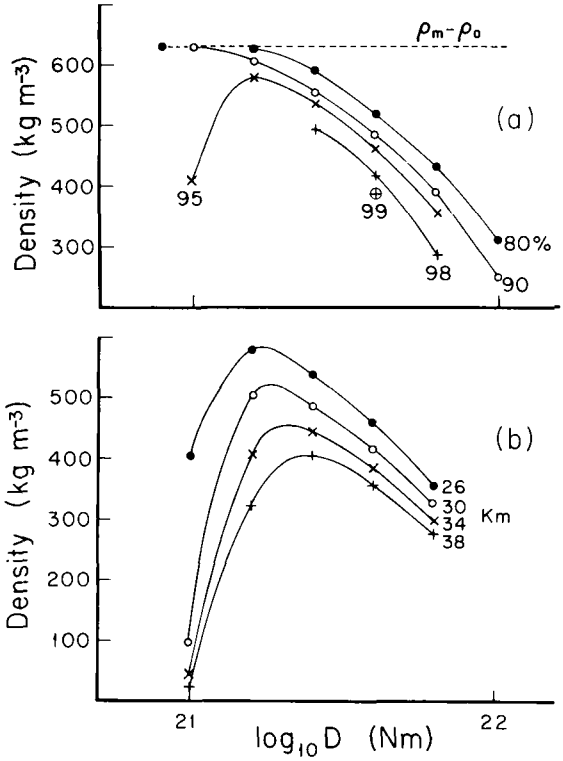

Figure 7. (a) Maximum density increase below 26 km as a function of the flexural rigidity (D). Curves correspond to different allowed misfits to the data. (b) Maximum density increase at or below different depths, as a function of flexural rigidity (D). Models are constrained to fit the data at the 95 per cent level.

on the density contrast at the Moho by finding the models that have the greatest and least total density increase ρ_s at depths of 26 km or more. The minimum value of ρ_s turns out to be zero, whatever the value of D. The maximum value is plotted in Fig. 7(a) as a function of the flexural rigidity, for different values of the misfit γ. In the previous section, we suggested that a misfit of 9.48 or less, corresponding to $P = 0.95$, was necessary for the model to be acceptable. With this choice, the maximum bound on the total density increase at or below 26 km is approximately 580 kg m^{-3}.

Twenty-six kilometres represents a minimum estimate of the Moho depth beneath the continents. If the depth is increased, the allowable density change is reduced. Fig. 7(b) shows the maximum allowed total density below different levels, plotted as a function of D. All the models are constrained to have a misfit to the data of 9.48 or less. If we have confidence that the Moho depth is 34 km or more, Fig. 7(b) tells us that the density contrast at the Moho must not exceed 470 kg m^{-3}. The other possible way of estimating the density difference between crust and mantle is from the seismic velocity structure, making use of the empirical relationship between P-wave velocity and density. However, interpretations of seismic refraction experiments conventionally assume that the crust is composed of a small number (generally not more than two) of layers of uniform velocity, and do not allow for the possibility of continuous vertical velocity gradients. Such interpretations can therefore only yield a maximum bound on the velocity contrast, which turns out to be approximately 1.5 km/s. The corresponding upper limit on the density contrast is 500 kg m^{-3}, which is even more liberal than our estimate. If it were possible to tighten the bound on the density

contrast, it would help to establish the reality of vertical density gradients in the lower crust. However, as it is, it is reassuring to find that regional compensation models that fit the data at a satisfactory level are compatible with density distributions derived in an entirely different way.

5 Discussion

We have shown that no local compensation model that involves only negative density contrasts beneath topographic loads fits the isostatic response function for the United States. Any form of local compensation, whether of the Airy or Pratt kind, can be dismissed if we are prepared to deny the reality of the positive density contrasts that are required to achieve an acceptable fit. For our part, we prefer to interpret the positive densities as an indication that the compensation mechanism is regional rather than local in character. We have studied a simple regional compensation model that treats the lithosphere as a thin elastic plate overlying a liquid. Only positive vertical density gradients are allowed in the plate. Such a model fits the United States response, provided the flexural rigidity of the plate lies in the range 10^{21}–10^{22} N m. The constraints that must be placed on the density structure of the plate in order to achieve an acceptable fit are compatible with what we know it to be from other geophysical measurements.

The bounds thus established on the flexural rigidity of the lithosphere deserve some comment. If the lithosphere really is a homogeneous and perfectly elastic plate, the seismically determined values of E and σ can be substituted into equation (9), and bounds placed on the plate thickness T. If $E = 9.2 \times 10^{10}$ N m^{-2}, $\sigma = 0.267$ (Bullen 1975), T must lie between 5.0 and 10.7 km. Such a result might suggest that we ought to constrain all our models to have zero density gradients below 11 km. It is certainly possible to find acceptable models that only involve such shallow compensating densities. However, seismic refraction experiments have shown that the depth of the Moho beneath the United States roughly mirrors the topography (e.g. Pakiser & Zietz 1965), so that deformations must be taking place in response to surface loads at depths of 30–40 km. It is not easy to determine whether deformation is also occurring at greater depths, because density and seismic velocity gradients in the upper mantle between 40 and 100 km depth are small. With this limitation in mind, it would appear from Fig. 8 that the isostatic response data are incompatible with density anomalies below about 80 km.

If the lithosphere is defined to be that part of the crust and upper mantle which deforms in response to surface loads, its thickness must be at least 30 or 40 km; much greater than the value obtained by assuming it to be elastic. It follows that the lithosphere does not behave as a homogeneous elastic plate in response to long term loading. The elastic plate model, with seismically determined elastic parameters, has been used to estimate the maximum stress difference within the Earth caused by topographic loading (e.g. Jeffreys 1970). Such an approach leads to values of several kilobars for the maximum stress difference. Our results indicate that these estimates are too large by a factor of four or more, because of the inadequacy of the rheological model. This lower value for the tectonic stress is much more nearly comparable with the stress drops in earthquakes as estimated by seismic studies (Brune 1971).

Walcott (1970, 1976) has proposed that the lithosphere be treated as a uniform visco-elastic plate with the properties of a Maxwell solid. The deformation in response to topographic loads is then time-dependent; the instantaneous response is elastic, and the compensation regional, but viscous flow leads ultimately to perfect local compensation. If such a model is correct, measurements of the deformation of the lithosphere in response to

loading will only yield apparent values of the flexural rigidity, which will decrease with the time that has elapsed since loading, i.e. according to the age of the topography. Walcott has made a number of estimates of D for topographic features in different parts of North America. In most cases, the deformation he measures is at the surface, and is assumed to have been caused by a topographic load that had subsequently disappeared, e.g. lakes such as Bonneville and Agassiz. His estimates of D range from 5×10^{22} N m (Lake Bonneville) to 9×10^{24} N m (Lake Agassiz), and a plot of D against the estimated age of the load does show an apparent decrease with elapsed time.

The effective age of topographic features in the United States may range from zero to more than 100 Myr. According to Fig. 5 of Walcott's (1970) paper, the corresponding range of values of D is from 10^{25} to 10^{22} N m. The effect of the variation should be to produce large standard errors in the response data, particularly at the wavelengths at which the isostatic response curve rolls off. The observed errors are, in fact, relatively small. A possible reason might be that the dominant topography of the western United States is of relatively uniform age. Even within this region, however, a considerable spread of ages still seems probable. Altogether, we dislike explanations of the observed response that rely on a fortuitous combination of widely different local circumstances.

We prefer an explanation that involves laterally consistent vertical variations in the rheology of the crust and mantle. The discrepancy between our estimate of D and those made by Walcott could arise from the different methods used to determine the deformation. In most of the examples he analyses, the deformation is measured at the surface, whereas ours is measured at depth by means of the gravity anomaly it produces. The lower value of D that we obtain could be taken to imply that the deformations associated with topographic loading are greater at depth than at the surface. This could be because the surface deformation had remained constant, and still represented the 'instantaneous' elastic value, whereas below 10 km, the initial elastic deformation had been converted by creep into that appropriate to local compensation. Thus we would favour a model with an elastic surface layer up to 10 km thick and with finite creep strength, rather than treat the entire lithosphere as a visco-elastic slab with, presumably, zero creep strength.

There is still considerable scope for improvement, both in the theory and the data. Further developments could include the use of a spherical earth model, 'thick plate' treatment of the loading problem, and the use of more realistic rheological models. Estimates of the isostatic response at shorter wavelengths would help to place tighter limits on both the flexural rigidity and the density structure.

Acknowledgments

We thank Marcia McNutt for computing the tables of the probability distribution for the one-norm. Computations were paid for by a grant from the National Science Foundation. RJB would like to thank the Green Foundation for contributing to his support while on sabbatical leave at IGPP.

References

Banks, R. J. & Swain, C., 1977. Isostatic compensation of the Kenya dome, *submitted.*

Brune, J. N., 1971. Seismic sources, fault plane studies and tectonics, *EOS Trans. Am. geophys. Un.*, **52**, 178–187.

Bullen, K. E., 1975. *The Earth's density*, Chapman & Hall, London.

Dorman, L. M. & Lewis, B. T. R., 1970. Experimental isostasy. 1: Theory of the determination of the Earth's isostatic response to a concentrated load, *J. geophys. Res.*, **75**, 3357–3365.

Dorman, L. M. & Lewis, B. T. R., 1972. Experimental isostasy. 3: Inversion of the isostatic Green function and lateral density changes, *J. geophys. Res.*, **77**, 3068–3077.

Gass, S. I., 1975. *Linear programming: methods and applications*, McGraw-Hill.

Hartley, H. O., 1945. Note on the calculation of the distribution of the estimate of mean deviation in normal samples, *Biometrika*, **33**, 257–258.

Hartley, H. O. & Godwin, H. J., 1945. Tables of the probability integral of the mean deviation in normal samples, *Biometrika*, **33**, 259–265.

Hayford, J. F. & Bowie, W., 1912. The effect of topography and isostatic compensation upon the intensity of gravity, *US Coast & Geodetic Survey Sp. Publn. No. 10.*

Heiskanen, W. A. & Vening Meinesz, F. A., 1958. *The Earth and its gravity field*, McGraw-Hill.

Jeffreys, H., 1970. *The Earth*, 5th edn, Cambridge University Press.

Lewis, B. T. R. & Dorman, L. M., 1970. Experimental isostasy. 2: An isostatic model for the U.S.A. derived from gravity and topographic data, *J. geophys. Res.*, **75**, 3367–3386.

McKenzie, D. P. & Bowin, C., 1976. The relationship between bathymetry and gravity in the Atlantic Ocean, *J. geophys. Res.*, **81**, 1903–1915.

Pakiser, L. C. & Zietz, I., 1965. Transcontinental crustal and upper mantle structure, *Rev. Geophys.*, **3**, 505–520.

Parker, R. L., 1973. The rapid calculation of potential anomalies, *Geophys. J. R. astr. Soc.*, **31**, 447–455.

Parker, R. L., 1975. The theory of ideal bodies for gravity interpretation, *Geophys. J. R. astr. Soc.*, **42**, 315–334.

Parker, R. L., 1977. Understanding inverse theory, *A. Rev. Earth planet Sci.*, **5**, 35–64.

Walcott, R. I., 1970. Flexural rigidity, thickness, and viscosity of the lithosphere, *J. geophys. Res.*, **75**, 3941–3954.

Walcott, R. I., 1976. Lithospheric flexure, analysis of gravity anomalies, and the propagation of seamount chains, *Am. geophys. Un. geophys. Monogr. 19*, 431–438.

Woollard, G. P., 1970. Evaluation of the isostatic mechanism and role of mineralogical transformations from seismic and gravity data, *Phys. Earth planet. Int.*, **3**, 484–498.